SPE-208632-STU

Reconstruction and Synthesis of Source Rock Images at the Pore Scale

Timothy Anderson, Stanford University

This paper was prepared for presentation at the SPE International Student Paper Contest at the SPE Annual Technical Conference and Exhibition held in Dubai, UAE, 21 - 23 September 2021.

Abstract

Image-based characterization of rock fabric is critical for understanding recovery mechanisms in shale formations due to the significant multiscale nature of shale source rocks. Nanoscale imaging is particularly important for characterizing pore-scale structure of shales. Nanoimaging techniques, however, have a tradeoff between high-resolution/high-contrast sample-destructive imaging modalities and low-contrast/low-resolution sample-preserving modalities. Furthermore, acquisition of nanoscale images is often time-consuming, expensive, and requires signficant levels of expertise, resulting in small image datasets that do not allow for accurate quantification of petrophysical or morphological properties. In this work, we introduce methods for overcoming these challenges in image-based characterization of the fabric of shale source rocks using deep learning models. We present a multimodal/multiscale imaging and characterization workflow for enhancing non-destructive microscopy images of shale. We develop training methods for predicting 3D image volumes from 2D training data and simulate flow through the predicted shale volumes. We then present a novel method for synthesizing porous media images using generative flow models. We apply this method to several datasets, including grayscale and multimodal 3D image volume generation from 2D training images. Results from this work show that the proposed image reconstruction and generation approaches produce realistic pore-scale 3D volumes of shale source rocks even when only 2D image data is available. The models proposed here enable new capabilities for non-destructive imaging of source rocks and we hope will improve our ability to characterize pore-scale properties and phenomena in shales using image data.

Introduction

Shale gas resources are critical for the U.S. energy supply: since 2009, a majority of the increase in domestic energy production has been due to shale gas (Zoback & Kohli 2019, EIA). With a growing interest in combining fossil energy recovery with implementation of sustainability technologies, shale plays and other unconventional reservoirs also present opportunities for use in subsurface CO_2 sequestration or H_2 storage (Hassanpouryouzband et al. 2021). Shales are exceptionally multiscale source rocks, where the interplay of features from $O(10^{-9}$ m) to $O(10^{2+}$ m) affects transport and recovery mechanisms, and therefore present many challenges for fully characterizing a reservoir (Mehmani et al. 2020).

Image-based characterization combined with digital rock physics techniques offer a powerful approach for understanding recovery mechanisms at the rock fabric scale in shales and connecting physics across length scales (Ketcham & Carlson 2001, Vega et al. 2013, Blunt 2017). Figure 1 shows rock features of shales and imaging modalities across length scales. Imaging data is able to connect physical information across modalities and length scales by acquiring images from different modalities or resolution scales and using digital rock physics to connect the images to petrophysical properties (Mehmani et al. 2020). This connection, however, requires the development of data-driven scale translation techniques, including upscaling, downscaling, translation, and generation (Anderson 2021).

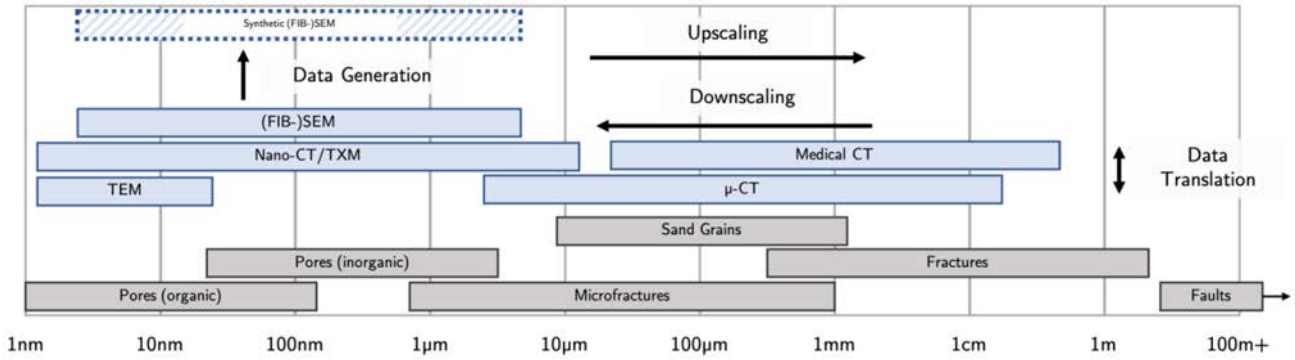

Figure 1—Scale and modality translation in image-based characterization of source rocks, including imaging modalities (blue), rock features (gray), and data-driven scale translation methods including data upscaling, downscaling, translation, and generation. ***Adapted from*** **Kohli (2015).**

One particularly promising application of data-driven scale translation techniques is to nanoscale imaging. Nanoscale imaging is particularly important for studying shales due to the importance of nanoporosity in shale gas storage. Nanoimaging techniques, however, present a tradeoff between high-resolution/high-contrast sample-destructive imaging modalities and low-contrast/low-resolution sample-preserving modalities. Acquisition of nanoscale images is also often time-consuming, expensive, and requires much expertise, resulting in small image datasets that do not allow for accurate quantification of petrophysical or morphological properties. Consequently, data translation and generation both offer many opportunities to assimilate multiple nano- and microscale modalities and overcome tradeoffs presented by nanoimaging systems.

Here we propose an image-based characterization workflow (Fig. 2) for data-driven scale translation that uses deep learning image synthesis and translation models to assimilate multimodal, multiscale, and data-scarce source rock images for predicting petrophysical and morphological properties. A central challenge in source rock characterization addressed in this work is the reconstruction of 3D volumes when only 2D training images are available. We present image translation models for reconstruction of 3D image volumes from 2D training data and a porous media image synthesis algorithm that generalizes to 3D grayscale and multimodal volume generation from 2D training data. In what follows, we describe the translation and synthesis models, apply these models to source rock image datasets, and discuss extensions and future directions for the workflow introduced here.

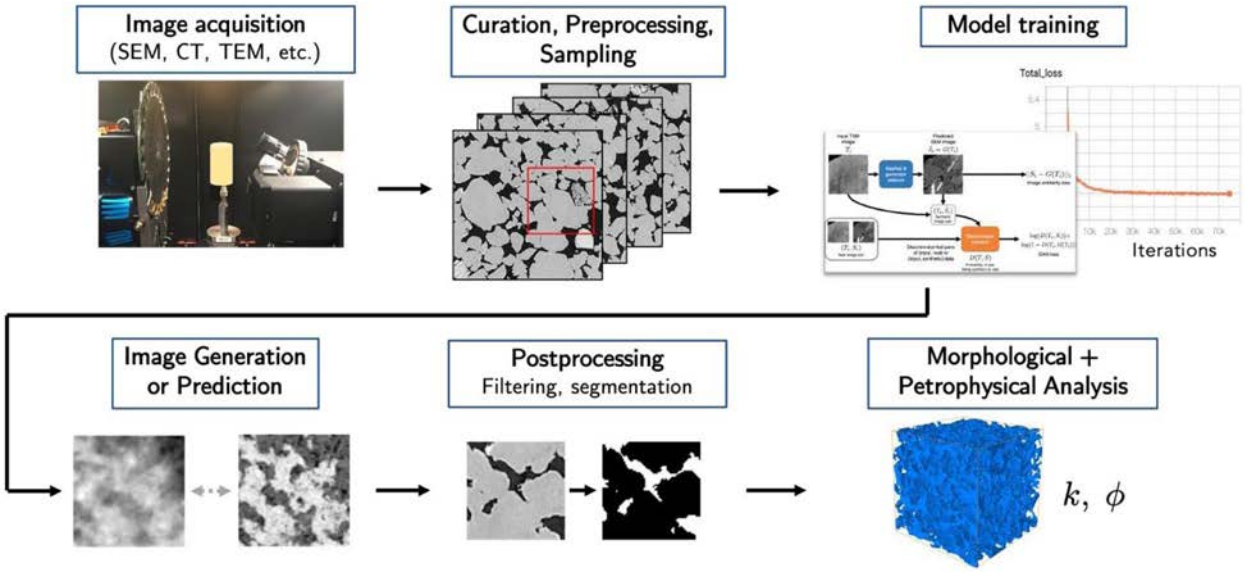

Figure 2—Image-based characterization and deep learning workflow. Images are first acquired for a source rock sample from one or multiple modalities. The image data is then curated, including alignment, normalization, and subsampling, to create a dataset suitable for machine learning model training. After training the image processing model, new images are generated or predicted. The synthesized images are post processed, including segmentation into pore and mineral phases, and the morphological and petrophysical properties of the sample evaluated.

Image Modality Translation

Multimodal imaging is an emerging approach for shale source rock characterization where images from multiple modalities at approximately the same resolution are acquired and assimilated to study a source rock sample. (Aljamaan et al. 2017). While multimodal imaging is common in medical imaging (Torrado-Carvajal et al. 2016, Cao et al. 2018, Zaharchuk et al. 2018), there exists no prior work applying multimodal imaging to shale characterization (Anderson et al. 2020). One potential application of multimodal imaging is training models to predict high-resolution/high-contrast destructive images from nondestructive input data. Such a setup allows for enhanced nanoscale characterization of a source rock sample while preserving the sample for further experimentation.

Towards developing shale image translation models, we use a dual-modality transmission X-ray microscopy (TXM) and focused ion beam-scanning electron microscopy (FIB-SEM) dataset presented in Anderson et al. (2020). This dataset consists of paired 2D TXM and FIB-SEM images of a Vaca Muerta shale sample acquired at 33.6 nm/px resolution. Example images from this dataset are shown in Fig. 3. FIB-SEM images offer very high resolution and contrast but require destruction of the sample during acquisition (Sondergeld et al. 2010). TXM images, meanwhile, are acquired non-destructively but offer reduced resolution and contrast compared to FIB-SEM imaging.

A key challenge in image translation from multimodal imaging is obtaining suitable aligned image data for training image prediction models. Image pairing and registration is difficult for multimodal images because the significant differences in image contrast and features between modalities do not allow for direct application of many automated registration algorithms. Furthermore, images are often also acquired on different grids. For the dataset considered here, the TXM image voxels are acquired on a three dimensional isotropic Cartesian grid while the FIB-SEM images are acquired with isotropic resolution in the x-y plane but irregular intervals in the z-direction. Well-aligned, normalized, paired images are required for image-to-image translation models, and consequently dataset preparation for multimodal imaging often requires a significant amount of manual data curation.

To predict FIB-SEM images from TXM input data, we use deep learning image translation and single image super resolution models (Ledig et al. 2016, Isola et al. 2017, Zhu et al. 2017). Due to the

differences in contrast and effective resolution of the TXM and SEM images, predicting FIB-SEM images involves elements of image translation and super-resolution. We explore two types of models for this task: feedforward convolutional neural network (CNN) models and generative adversarial network (GAN) models. For both families of models, we consider models that map a full-resolution TXM image to a full-resolution SEM image and a super-resolution version of the model that upsamples a synthetically-downsampled TXM image to the target SEM image.

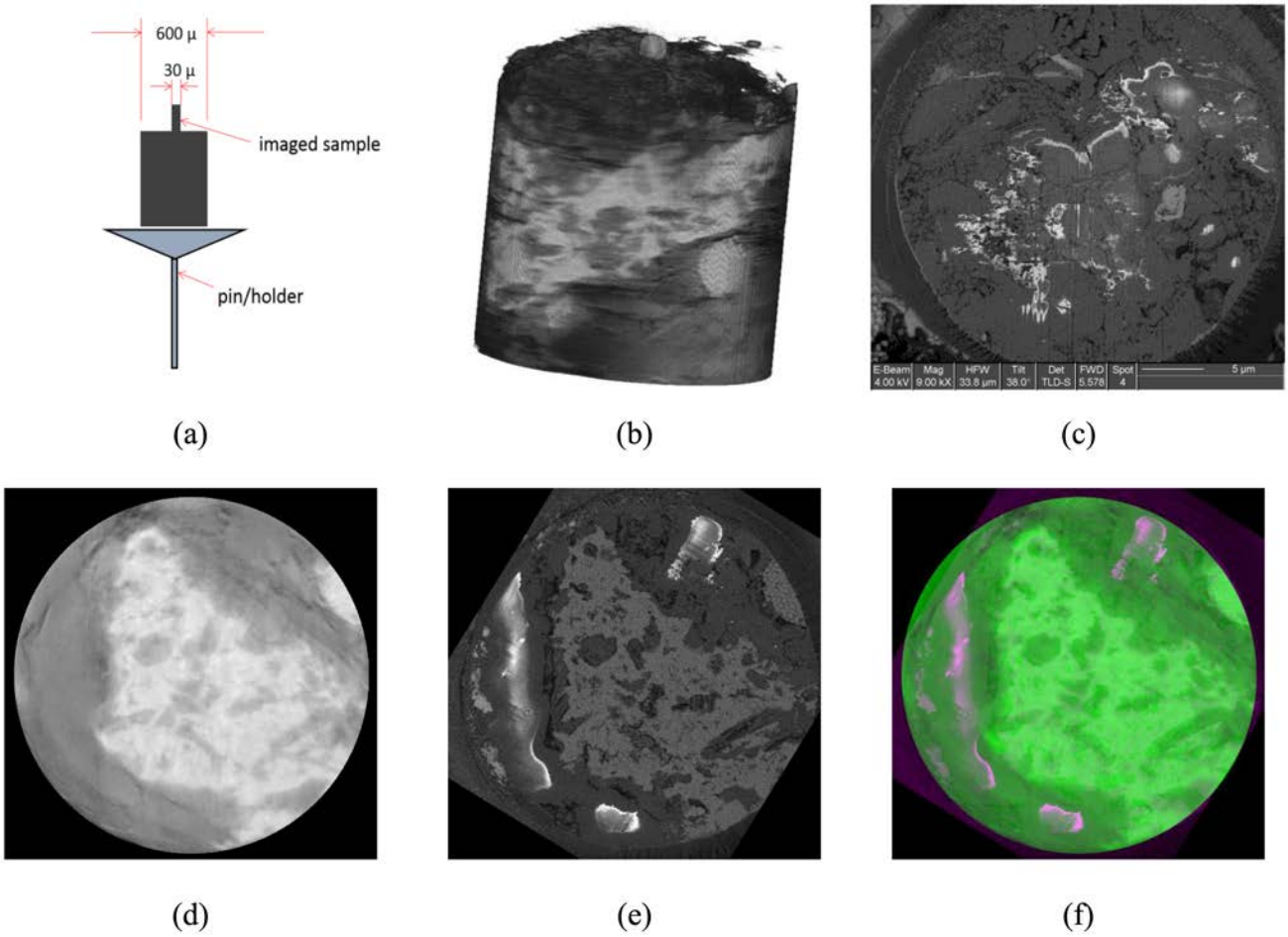

Figure 3—Multimodal image dataset of Vaca Muerta shale sample. (a) Sample setup: after initial imaging using µ-CT, the core is milled down to a 600µm diameter core with a 30 µm protruding plug. (b) Imaged TXM volume of 30 µm diameter plug. (c) Unprocessed FIB-SEM image slice at acquisition. The sample is milled down using FIB milling and successive x-y image slices of the volume are acquired using SEM imaging. (d-e) Example of paired (d) TXM and (e) FIB-SEM image slices after pairing, alignment, and normalization. (f) Overlayed paired image slice with TXM shown in green and FIB-SEM shown in magenta.

CNN models train a generator network $G(\cdot)$ to map the input TXM image T to an output FIB-SEM image $\hat{S} = G(T)$ according to the objective function:

$$G^* = \arg\min_G \sum_{T,S} g\left|G(T) - S\right|_1$$

where (T, S) is a TXM/SEM image pair from the dataset. We also use the pix2pix conditional GAN (CGAN) model from Isola et al. (2017) and the SRGAN model from Ledig et al. (2016). These image translation models train a generator network $G(\cdot)$ as well as a discriminator network $D(\cdot)$. GAN-based models create a feedback loop between the generator and discriminator networks that encourages the generator to create more natural-looking images (Ledig et al. 2016). The image translation models are trained according to:

$$G^* = \arg\min_G \max_D \sum_{(T,S)} g\mathcal{L}_{\text{GAN}}(G(T), S) + \lambda|G(T) - S|_1$$

where $\mathcal{L}_{\text{GAN}}(\cdot)$ is the training loss function for a given GAN model. Here we consider the vanilla GAN and Wasserstein GAN losses (Goodfellow et al. 2014, Arjovsky et al. 2017, Gulrajani et al. 2017). The CNN and CGAN models, as well as the network architecture used for the generator network $G(\cdot)$ are shown in Fig. 4.

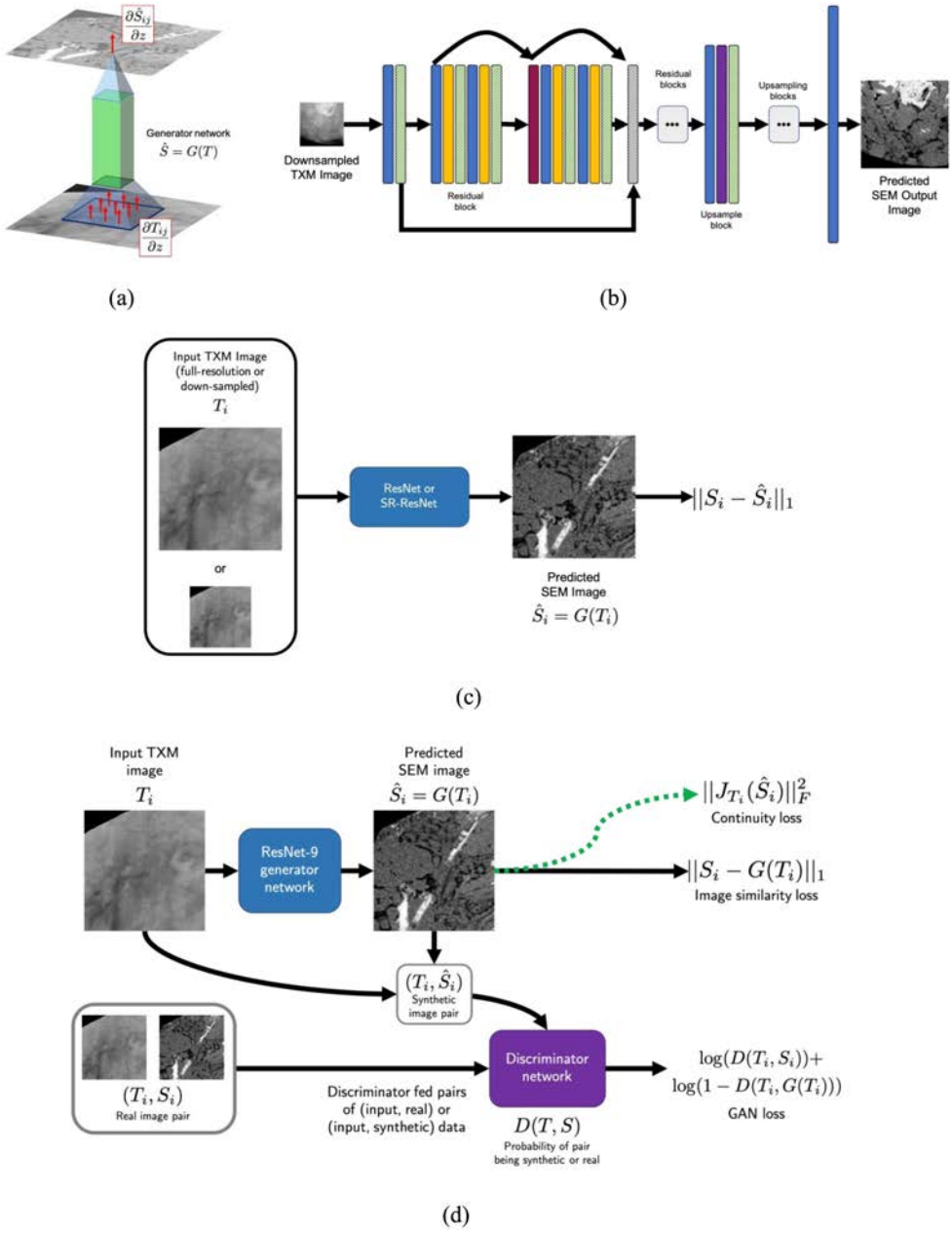

Figure 4—(a) The z-direction gradient for a voxel of the predicted SEM image $\hat{S}$ is affected by the z-gradients for all TXM voxels within the field of view. (b) SR-ResNet architecture from Ledig et al. (2016). ResNet architectures are characterized by blocks of network layers with skip connections between layers. The ResNet-9 architecture used in the CGAN and CNN models are similar to the SR-ResNet shown here. (c) Feedforward model: a full-resolution or downsampled TXM image to predict the corresponding SEM image. (d) pix2pix CGAN model: a full-resolution TXM image is used to predict an SEM image. The TXM image and predicted SEM image are then fed into a discriminator network to calculate the probability that the pair is real or synthetic. The SR-GAN model follows a similar architecture with modifications to the generator network and input to the discriminator.

Results from the 2D-to-2D image translation models are shown in Fig. 5 for feedforward CNN, pix2pix CGAN model with vanilla GAN loss, and SRGAN models with 4x and 2x upsampling factors. These models were chosen because they provide the best contrast in results between the various models considered for this study. We measure model performance according to three metrics: peak signal-to-noise ratio (PSNR), structural similarity index metric (SSIM), and structural texture similarity index metric (STSIM), a modification of SSIM that measures the perceptual similarity of two images (Zhao et al. 2008). From the example images, we see that the pix2pix models have the best performance in terms of PSNR and SSIM, while the SRGAN model performs best in terms of STSIM.

To characterize fully the morphological and petrophysical properties of a sample, we require a translated 3D image volume. Traditionally, 3D-to-3D models require 3D training data. In multimodal shale imaging, however, at least one of the imaging modalities—for example, electron microscopy-based modalities—will often only acquire 2D images, and therefore available training data will only be in 2D. To extend 2D data to 3D-to-3D generation, we propose a novel regularization method to enforce continuity between adjacent image slices in the translated image volume. We assume that the z-direction gradients for the predicted SEM image $\nabla_z \hat{S}$ are sparse, so using the property:

$$\left|\nabla_z \hat{S}\right|_1 \le \left|\frac{\partial \hat{S}}{\partial T}\right|_F \equiv \mathcal{L}_{Continuity}(G(T))$$

we can encourage the generator to synthesize image volumes with z-direction continuity by regularizing the 2D-to-2D model training:

$$G^* = \arg\min_G \sum_{(T,S)} \mathcal{L}(G(T), S) + \mathcal{L}_{Continuity}(G(T))$$

where $\mathcal{L}(G(T), S)$ is the original loss function.

Results from translating image volumes with baseline and regularized SR-GAN 4x models are shown in Fig. 6a-c. The volumes are 128^3 voxels and generated by independently evaluating each 128x128 px x-y image slice and concatenating in the z-direction to form the image volume. From the predicted images, we see that the Jacobian regularization term significantly improves the continuity of features between successive x-y image slices.

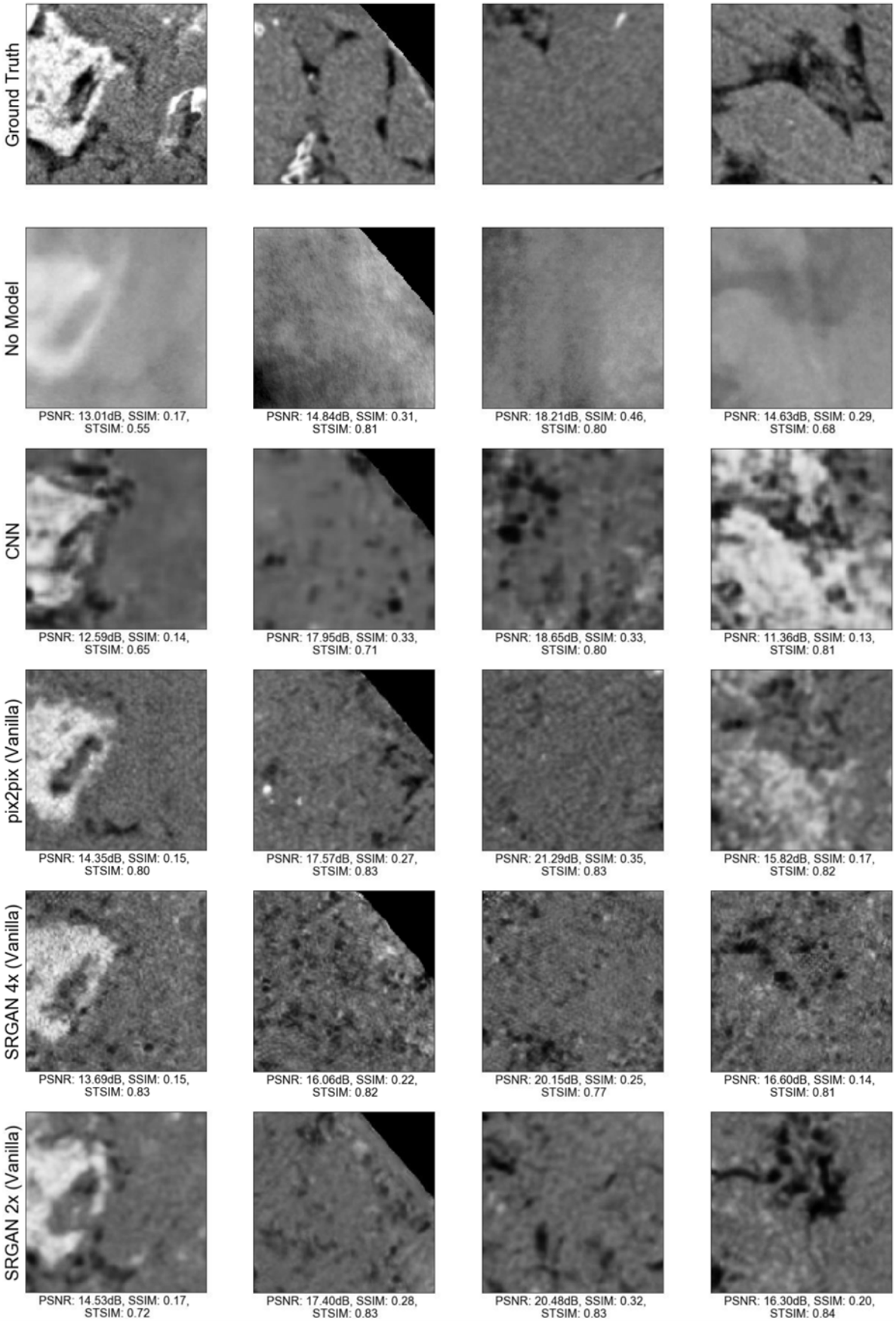

Figure 5—Example test set images for 2D-to-2D image prediction models considered here.

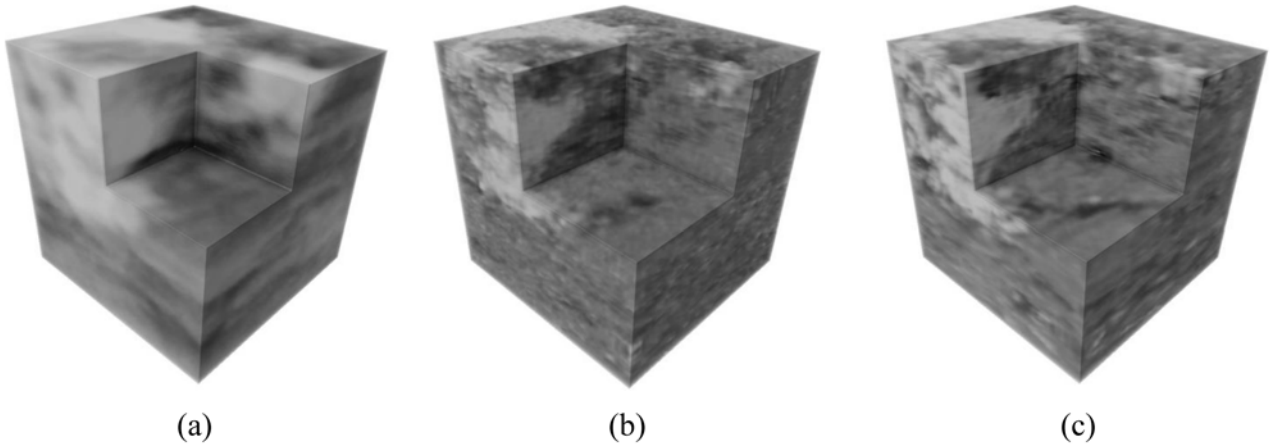

Figure 6—(a) TXM image volume, (b) Predicted FIB-SEM volume with SRGAN model, (c) Predicted FIB-SEM volume with regularized SRGAN model. The regularized image volume shows improved continuity of rock features between adjacent image slices.

After synthesizing the image volumes, we segment the volumes into a simulation domain to calculate the apparent permeability. We create the simulation domain (Fig. 7a) by segmenting the lower density regions of the synthesized image volume using thresholding-based segmentation and discarding any disconnected regions. We then compute the pressure field (Fig. 7b) and flow streamlines (Fig. 7c) using the PerGeos software package. We find permeability $\varphi = 2.37 \times 10^{-5}$ d for the image volume generated with the baseline SRGAN model (Fig. 6b) and $\varphi = 3.01 \times 10^{-5}$ d for the volume from the regularized SRGAN model (Fig. 6c). While these values are higher than expected for shale volumes at the rock fabric scale, these results demonstrate that we are able to visualize flow through the rock volume using entirely nondestructive imaging techniques combined with image translation models.

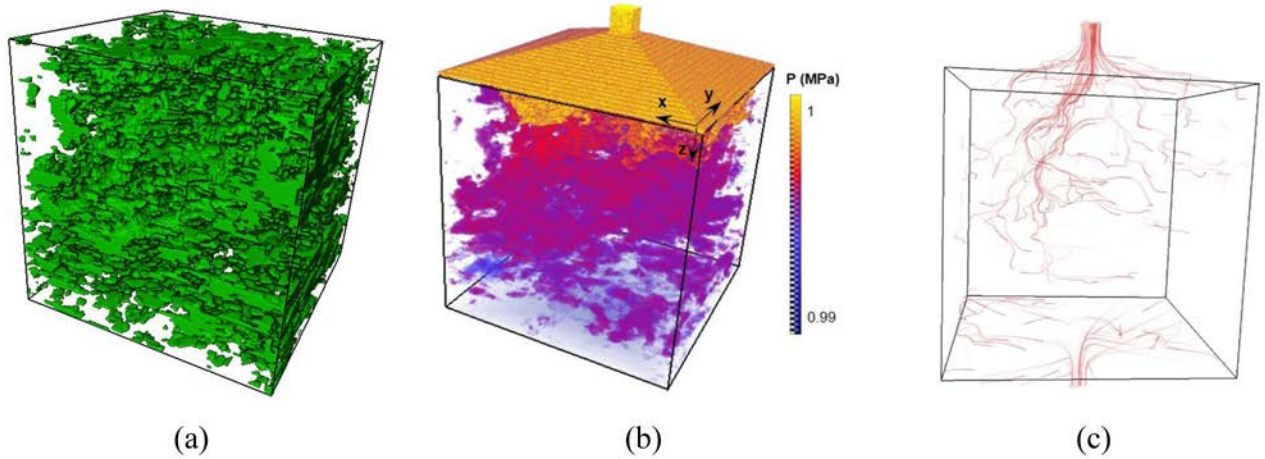

Figure 7—Results from simulation of methane flow through the predicted rock volume. (a) Low-density regions (kerogen, porosity, low-density minerals) segmented using thresholding-based segmentation. (b) Pressure field resulting from injecting methane into the reconstructed volume with inlet pressure 1 MPa and a pressure drop of 10^{-2} MPa. (c) Flow streamlines traced through the rock volume. The flow results show that the presented characterization workflow allows for computation of petrophysical properties and visualization of flow through rock volumes using entirely non-destructive imaging data.

Porous Media Image Synthesis

Another challenge for image-based characterization of porous media is data scarcity due to the time-consuming, costly, or sample-destructive nature of many nanoimaging techniques. One approach that has been proposed to address data scarcity is to train a generative model to synthesize images of porous media samples, then estimate the morphological or petrophysical properties by sampling synthetic images from

the generative model and computing properties for these images (Adler et al. 1990). Methods for porous media synthesis are approximately divided into statistical methods that seek to replicate multipoint spatial statistics of samples or deep learning-based generative models (Roberts 1997, Manwart et al. 2000, Mosser et al. 2017). While existing methods have been very successful for many rock types, these approaches do not generalize to 3D grayscale volume generation from 2D images, and no existing work has explored multimodal/multiscale image volume generation.

Towards overcoming these limitations, we have developed a new method for synthesizing source rock images that is based on generative flow models (Dinh et al. 2015, Kingma & Dhariwal 2018). Generative flow models are a type of deep learning generative model that learns a bijective mapping $F(\cdot)$ between data points x_i and latent vectors $x_i = F(z_i)$ with known distribution $z_i \sim \#(\mu, \Sigma)$. Our method is based on the latent space interpolation property of generative flow models, where linear interpolation in the latent space produces semantic interpolation in the data space (Fig. 8a). We can use this property to synthesize porous media image volumes by sampling independent z_i vectors as "anchor slices," computing a linear combination between these latent vectors, then evaluating the anchor slices and interpolated vectors to create the x-y plane image slices for the image volume. The image generation process is shown in Fig. 8b and explained further in Anderson et al. (2020) and Guan et al. (2020). The x-y plane slice in Fig. 9a and x-z plane in Fig. 9b show that both the generated slices and cross-sections orthogonal to the image generation plane resemble images from the ground truth sample, but the cross-sectional slices display a jittering effect at the pore-grain phase boundaries. We find that applying a spherical median filter (Fig. 9c), however, significantly reduces this jittering between slices.

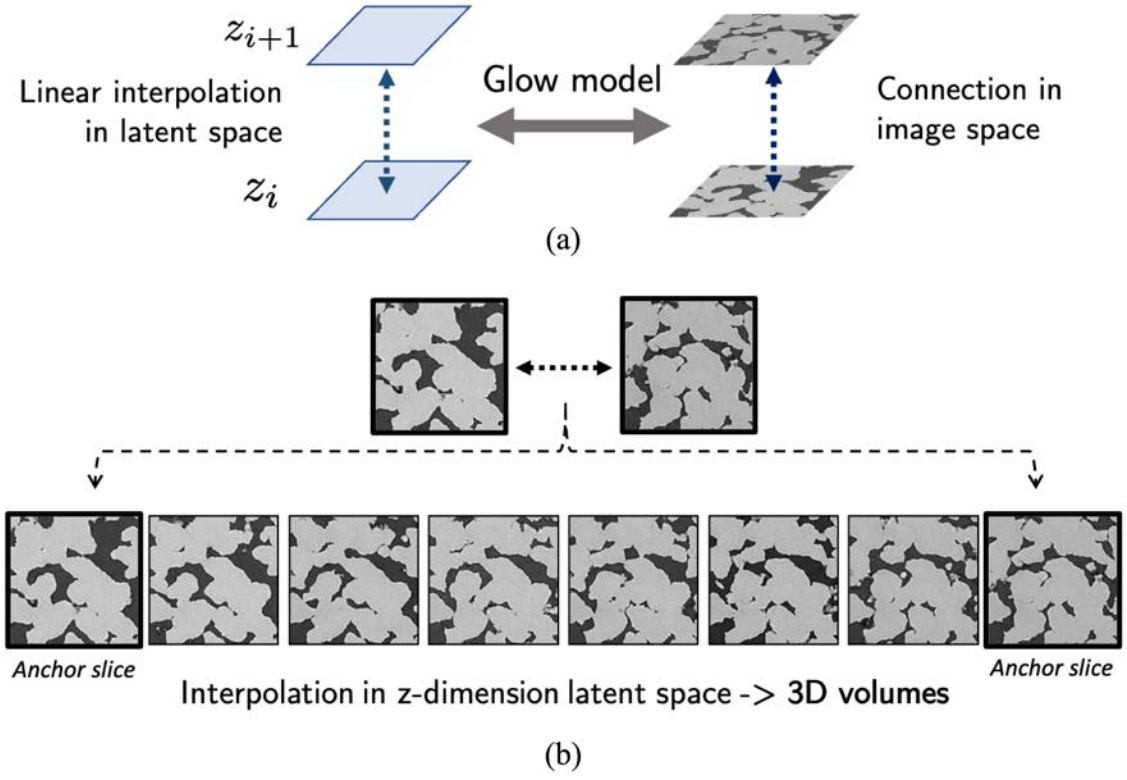

Figure 8—(a) Latent space interpolation property of generative flow models, (b) Overview of RockFlow algorithm. Anchor slices are sampled independently and the volume built by interpolating between anchor slices.

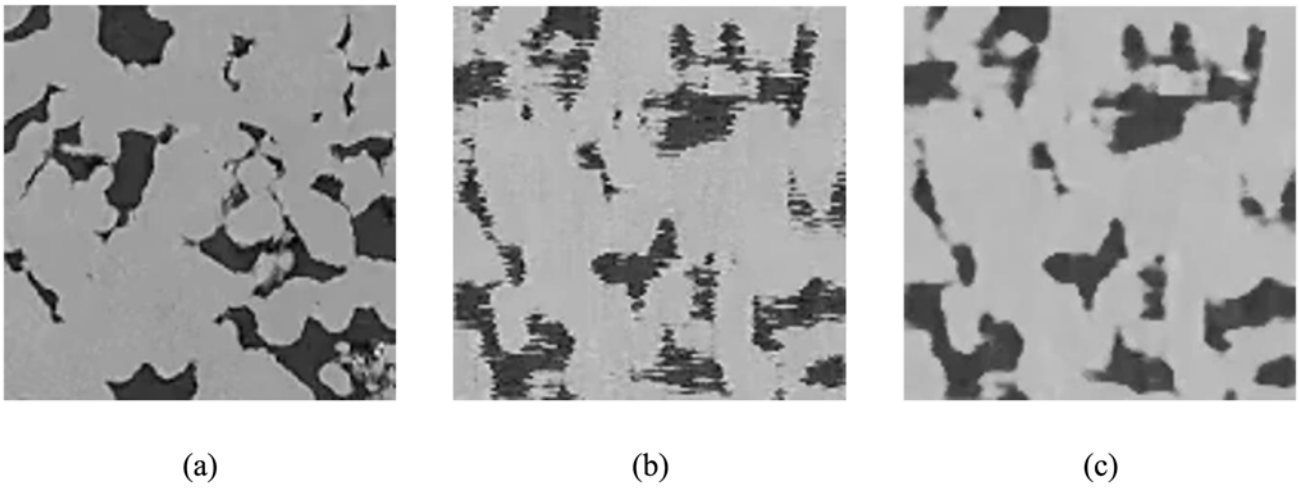

Figure 9—(a) x-y (image generation plane) slice, (b) x-z (orthogonal plane) slice, (c) x-z image slice after applying a spherical median filter.

We also apply this approach to multimodal image generation. In multimodal image generation, we treat each image modality as separate channels in the input image. A synthetic TXM/SEM volume, generated with a modified version of the Vaca Muerta multimodal image dataset, is shown in Fig. 10. The multimodal volume has similar image features in the x-y plane (image generation plane) as in the x-z and y-z planes, showing the ability of the proposed image generation algorithm to create realistic multimodal grayscale image volumes when only 2D training data is available.

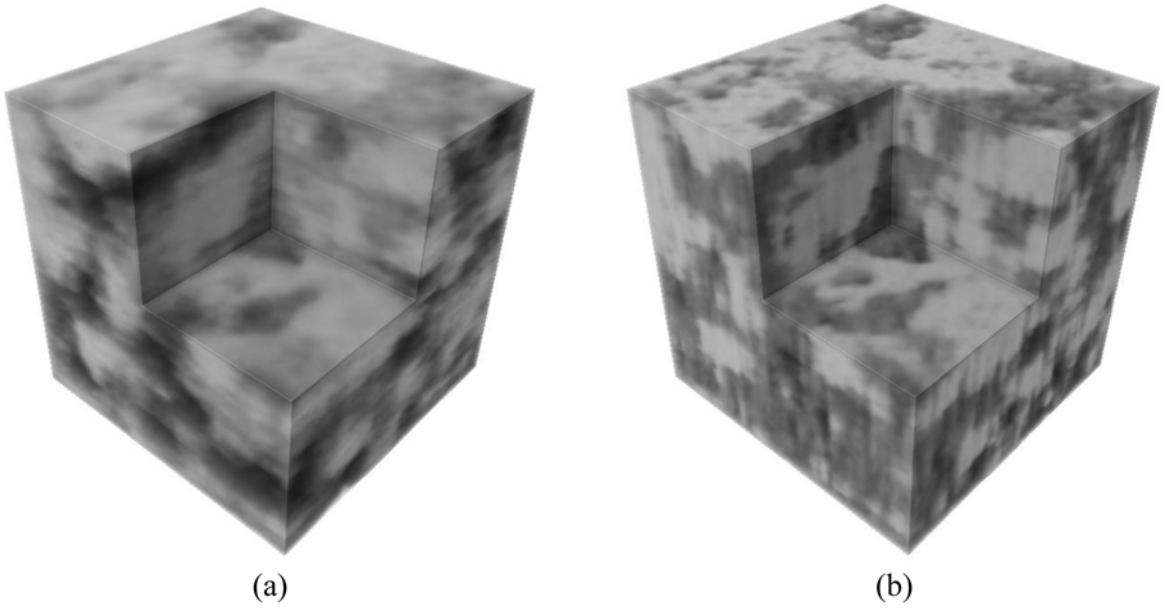

Figure 10—Synthesized multimodal grayscale image volumes from 2D training data. 128^3 voxel volume at 62.7^3 nm/voxel resolution. (a) Synthetic TXM volume, (b) Synthetic FIB-SEM volume post-processed with 1x1x3 median filter.

Conclusions and Future Work

The work presented here demonstrates the ability of deep learning generative models to enable new shale characterization methods. The proposed models overcome limitations of the imaging systems to create image volumes from 2D data and address data scarcity by generating realistic new data samples. The image translation results show that the addition of a Jacobian regularization term during training creates image

volumes suitable for flow simulations, and the data synthesis results show that the proposed algorithm creates accurate 3D volumes from 2D training data and generalizes to multimodal and grayscale generation.

Future work in shale image translation should focus on integration of unpaired imaging data into image translation workflows; such an approach would allow models to take advantage of the vast amount of unpaired source rock imaging data available. For data synthesis, future work should focus on quantifying uncertainty in rock properties using synthetic data (Guan et al. 2020). Nanoporosity data obtained from transmission electron microscopy images could also be combined with synthetic and translated rock volumes to create accurate pore networks in the lower density regions (Frouté et al. 2020). Such multiscale image volumes would allow for more accurate characterization of petrophysical properties of shales.

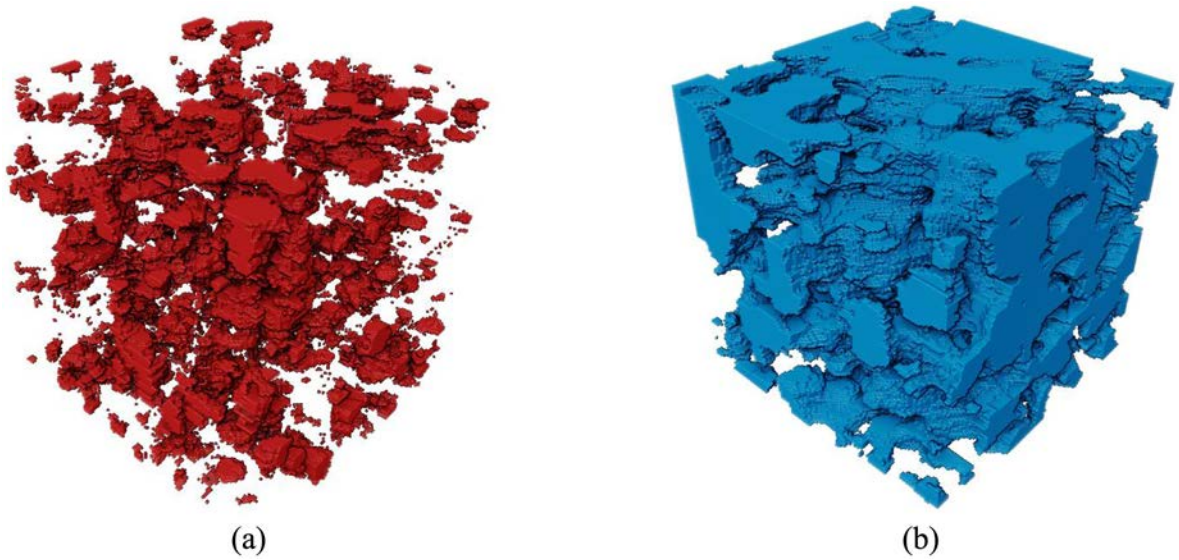

Figure 11—(a) Low density (kerogen, porosity, low-density minerals) and (b) high density region segmentations for the synthesized FIB-SEM volume shown in Fig. 10b. Segmented volumes from synthesized multimodal images can be used to calculate the distribution of petrophysical and morphological properties in a way similar to the approach used for image translation tasks.

Long term, there is the possibility of integrating image translation and generation models with other characterization tasks, as shown in Fig. 12. Neural network models learn hierarchical features of input images; in a ResNet architecture, for example, these are the feature maps in between successive residual blocks. A potential future direction would be to use networks pre-trained on image data, then use learned high-level representations of rock images to train models for other tasks such as data-driven simulation, predictive modeling and analysis, or transfer learning to other imaging tasks. Such an approach would provide many opportunities to link physics and imaging across length scales, and in turn further our understanding of shale source rocks.

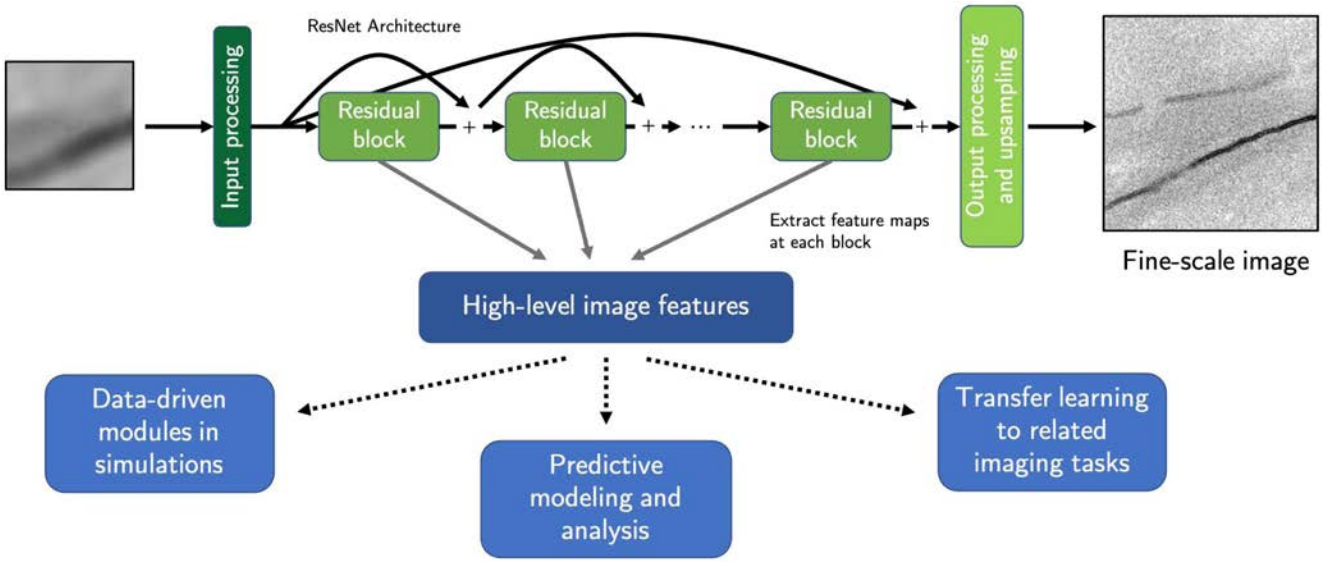

Figure 12—Learned multiscale/multimodal representations of source rock images have potential applications in other tasks including data-driven simulation, predictive modeling and analysis, and transfer learning to related tasks with data scarcity.

Acknowledgements and Code Release

Thank you to Anthony R. Kovscek, Kelly M. Guan, Bolivia Vega, Laura Frouté, Cynthia M. Ross, Jesse McKinzie, and Saman A. Aryana for their input and assistance with the work presented here. This work was supported as part of the Center for Mechanistic Control of Water-Hydrocarbon-Rock Interactions in Unconventional and Tight Oil Formations (CMC-UF), an Energy Frontier Research Center funded by the U.S. Department of Energy (DOE), Office of Science, Basic Energy Sciences (BES), under Award # DE-SC0019165. Part of this work was performed at SNSF on a ZEISS Xradia 520 Versa (NSF award CMMI-1532224). SNSF is supported by the NSF as part of the National Nanotechnology Coordinated Infrastructure under award ECCS-1542152. Many thanks to Total, Mathworks, and the SUPRI-A Industrial Affiliates for their generous support of this work. Timothy Anderson is also supported by the Siebel Scholars Foundation.

Code for this work is available at https://github.com/supri-a/TXM2SEM and https://github.com/supri-a/RockFlow. The code used here was adapted from the code provided by Isola et al. (2017), Zhu et al. (2017), Kingma and Dhariwal (2018), https://github.com/y0ast/Glow-PyTorch, and Mosser et al. (2017).

References

Adler, P.M., Jacquin, C.G., & Quiblier, J.A. (1990). Flow in simulated porous media. *International Journal of Multiphase Flow*, **16**(4), 691 - 712.

Aljamaan, H., Ross, C.M., Kovscek, A.R. (2017). Multiscale Imaging of Gas Storage in Shales. *SPE Journal*, **22**(06), 1–760.

Anderson, T. I., Guan, K. M., Vega, B., Aryana, S. A., & Kovscek, A. R. (2020). RockFlow: Fast Generation of Synthetic Source Rock Images Using Generative Flow Models. *Energies*, **13**(24), 6571.

Anderson, T. I., Vega, B., & Kovscek, A. R. (2020). Multimodal imaging and machine learning to enhance microscope images of shale. *Computers & Geosciences*, **145**, 104593.

Anderson, T. I. (2021). Data-driven methods in laboratory-scale study of enhanced oil recovery. (Doctoral dissertation, Stanford University).

Arjovsky, M., Chintala, S. & Bottou, L. Wasserstein GAN (2017). 1701.07875.

Blunt, M. (2017). Multiphase Flow in Permeable Media: A Pore-Scale Perspective. Cambridge University Press.

Cao, X. et al. (2018). Deep learning based inter-modality image registration supervised by intra-modality similarity. In International Workshop on Machine Learning in Medical Imaging (pp. 55–63).

Dinh, L., Krueger, D., & Bengio, Y. (2015). NICE: Non-linear independent components estimation. 3rd International Conference on Learning Representations, ICLR 2015 - Workshop Track Proceedings, **1**(2), 1–13.

EIA (2021). https://www.eia.gov/energyexplained/us-energy-facts/.
Frouté, L., Wang, Y., McKinzie, J., Aryana, S., & Kovscek, A. (2020). Transport Simulations on Scanning Transmission Electron Microscope Images of Nanoporous Shale. *Energies*, **13**(24), 6665.
Goodfellow, I. J. et al. Generative Adversarial Networks (2014). 1406.2661.
Guan, K., Anderson, T., Cruex, P., & Kovscek, A. (2020). Reconstructing Porous Media Using Generative Flow Networks. *Computers & Geosciences, in review*.
Gulrajani, I., Ahmed, F., Arjovsky, M., Dumoulin, V. & Courville, A. Improved Training of Wasserstein GANs (2017). 1704.00028.
Hassanpouryouzband, A., Joonaki, E., Edlmann, K., and Haszeldine, R. S. Offshore geological storage of hydrogen: Is this our best option to achieve net-zero? *ACS Energy Letters*, pp. 2181–2186, May 2021. doi: 10.1021/acsenergylett.1c00845.
Isola, P., Zhu, J.-Y., Zhou, T. & Efros, A. A. Image-to-image translation with conditional adversarial networks. In Proceedings of the IEEE conference on computer vision and pattern recognition, 1125–1134 (2017).
Ketcham, R., & Carlson, W. (2001). Acquisition, optimization and interpretation of x-ray computed tomographic imagery: Applications to the geosciences. *Computers and Geosciences*, **27**(4), 381–400.
Kingma, D., & Dhariwal, P. (2018). Glow: Generative flow with invertible 1x1 convolutions. *Advances in Neural Information Processing Systems*, 2018-Decem, 10215–10224.
Kohli, A. (2015). Micromechanical Controls on Brittle to Plastic Fault Zone Deformation. (Doctoral dissertation, Stanford University).
Ledig, C. et al. Photo-Realistic Single Image Super-Resolution Using a Generative Adversarial Network. arXiv DOI: 10.1109/CVPR.2017.19 (2016). 1609.04802.
Manwart, C., Torquato, S., & Hilfer, R. (2000). Stochastic reconstruction of sandstones. *Physical Review E - Statistical Physics, Plasmas, Fluids, and Related Interdisciplinary Topics*, **62**(1 B), 893–899.
Mehmani, Y. et al. (2020). Striving to Translate Shale Physics across Ten Orders of Magnitude: What Have We Learned?. *Earth-Science Reviews*, submitted.
Mosser, L., Dubrule, O., & Blunt, M. (2017). Reconstruction of three-dimensional porous media using generative adversarial neural networks. *Physical Review E*, **96**(4).
Okabe, H., & Blunt, M. (2004). Prediction of permeability for porous media reconstructed using multiple-point statistics. *Physical Review E - Statistical Physics, Plasmas, Fluids, and Related Interdisciplinary Topics*, **70**(6), 10.
Roberts, A. (1997). Statistical reconstruction of three-dimensional porous media from two-dimensional images. *Phys. Rev. E*, **56**, 3203–3212.
Sondergeld, J. et al. (2010). Micro-structural studies of gas shales. In SPE unconventional gas conference.
Torrado-Carvajal, A. et al. (2016). Fast Patch-Based Pseudo-CT Synthesis from T1-Weighted MR Images for PET/MR Attenuation Correction in Brain Studies. *Journal of Nuclear Medicine*, **57**(1), 136–143.
Vega, B. et al. (2013). Nanoscale visualization of gas shale pore and textural features. In Unconventional resources technology conference (pp. 1603–1613).
Zaharchuk, G. et al. (2018). Deep learning in neuroradiology. *American Journal of Neuroradiology*, **39**(10), 1776–1784.
Zhao, X., Reyes, M. G., Pappas, T. N. & Neuhoff, D. L. Structural texture similarity metrics for retrieval applications. In 2008 15th IEEE International Conference on Image Processing, 1196–1199.
Zhu, J. Y., Park, T., Isola, P. & Efros, A. A. Unpaired Image-to-Image Translation Using Cycle-Consistent Adversarial Networks. *Proc. IEEE Int. Conf. on Comput. Vis*. 2017-Octob, 2242–2251, DOI: 10.1109/ICCV.2017.244 (2017). 1703.10593.
Zoback, M., & Kohli, A. (2019). Unconventional reservoir geomechanics. Cambridge University Press.